



## EFFECT OF MECHANICAL ACTIVATION ON THE LEACHING CHARACTERISTICS OF INDIAN ILMENITE

C.Sasikumar<sup>1</sup>, S.Srikanth<sup>1</sup> and N.K.Mukhopadhyay<sup>2</sup>

<sup>1</sup> National Metallurgical Laboratory - Madras Centre  
CSIR Madras Complex, Post TTTI, Taramani  
Chennai – 600 113, INDIA

<sup>2</sup> Department of Metallurgy  
Institute of Technology, Banaras Hindu University  
Varanasi – 221 005, INDIA

### ABSTRACT

An ilmenite concentrate from chatapur, orissa India has been subjected to mechanical activation in a planetary mill. The effect of mechanical activation on the phase constitution, particle size and distribution, surface area, structural parameters, crystallite size and strain of a beach sand ilmenite concentrate and their effect on the kinetics of sulfuric acid leaching has been investigated. It was observed that mechanical activation significantly enhances the dissolution of both iron and titanium in sulfuric acid. The leaching behavior for both Ti and Fe showed a sigmoidal increase with time at all leaching temperatures in the range of 80-120°C and for all times activation. More than 65% of Ti and 90% of Fe could be dissolved at 120°C in four hours of leaching. The kinetic parameters for leaching of activated samples were determined using a non-linear least square minimization procedure. The activation energy for leaching of Fe and Ti decreased monotonically with activation time.

Keywords: Ilmenite, Mechanical activation, Sulphuric acid leaching, Kinetics

### 1. INTRODUCTION

Synthetic rutile (TiO<sub>2</sub>) plays an important role in production of paints, pigments, plastics and welding rod coatings. Ilmenite (FeO.TiO<sub>2</sub>) is one of the major resources of synthetic rutile. Indian coastal regions are enriched with ilmenite concentrate and it is estimated to be about 278 million tons around the coastal beach at Orissa, Tamilnadu and Kerala respectively. Ilmenite concentrate is upgraded by several methods to produce synthetic rutile. Acid leaching is one of the most common methods that produce high-grade synthetic rutile. However leaching is the slowest step, which determines the production rate. Several investigations have been carried out to enhance the dissolution rate of ilmenite. Most of the methods include high temperature oxidation/reduction pretreatment and high pressure leaching that involves high operating cost environmental and safety problems.

Mechanical activation introduces physical and structural changes thereby the leaching characteristics of minerals are enhanced even at ambient pressures. Amer, 2000; Ballaz et al., 1992; Ballaz, 1996, Tkacova and Balaz, 1996 studied about the mechanical activation of oxide and sulfide minerals. Welham and Llewellyn (1998), Welham, 2001, Amer (2002) and Sasikumar et al., 2004 carried out the detail investigation on mechanical activation and its influence on the leaching characteristics of ilmenite in sulfuric acid. They showed that mechanical activation significantly enhances the dissolution rate even at ambient pressure. The

enhancement of dissolution rate is attributed to increase in specific surface area of dissolution, change in morphology of the powder particles, structural disorder, amorphization and formation of new phases more amenable to leaching. Welham and Llewellyn (1998) suggested that using a vibratory mill could reduce the results obtained by 100 hours of ball milling.

In this paper the enhancement of dissolution rate of ilmenite by mechanical activation is investigated. The ilmenite sample is activated in a planetary mill and the effect of mechanical activation on particle size, surface area, morphology of the particles, crystallite size, strain and structural changes were investigated. The effect of mechanical activation on kinetic parameters is investigated by leaching with 50% sulfuric acid.

## 2.EXPERIMENTAL

### 2.1.Material

The ilmenite concentrate used in this study was obtained from Indian Rare Earths Limited, Chatrapur, Orissa, India. The bulk chemical composition shows 50.55%  $\text{TiO}_2$ , 34.20 %  $\text{FeO}$ , 12.30 %  $\text{Fe}_2\text{O}_3$ , 0.45%  $\text{Al}_2\text{O}_3$ , 0.70 %  $\text{SiO}_2$ , 0.54 %  $\text{MnO}$ , 0.23%  $\text{V}_2\text{O}_5$ , 0.05%  $\text{Cr}_2\text{O}_3$ , 0.05 %  $\text{CaO}$ , 0.72 %  $\text{MgO}$  and 0.02 % Rare Earths.. All the reagents used for chemical analysis were of analytical grade and of purity greater than 99.9%.

### 2.2.Mechanical Activation

The samples were activated in a Fritsch Pulviresette-5 planetary mill having agate bowl and balls (Fritsch GMBH, Germany). The mechanical activation has been carried out for 30, 90 and 240 minutes. The powder-to-ball ratio was maintained at 1:4 and the speed of milling is kept at 200rpm at reverse mode of rotation for all the batches of experiments. At the completion of grinding, the contents of the bowl were thoroughly cleaned and dried before the next milling experiment.

### 2.3.Characterization

The mechanically activated samples as well as the unmilled samples were characterized by XRD, optical and electron microscopy, particle size analysis and surface area measurement. X-ray diffraction studies were carried out in a Siemens D-500 diffractometer using  $\text{Co-K}\alpha$  radiation ( $\lambda=1.79026 \text{ \AA}$ ) at a scan rate of  $1^\circ/\text{min}$ , microstructural analysis using a LEITZ Orthoplan optical microscope and JEOL JSM 840A scanning electron microscope in the back-scatter electron imaging mode, EPMA analysis using a JEOL, Super Probe JXA-8600 model electron microprobe operating with a current setting of  $2 \times 10^{-8} \text{ A}$ , with Standard Programme International (SPI) mineral standards and using on-line ZAF correction procedures, particle size analysis using a laser diffraction analyzer (CILAS 1180, France) and surface area measurements using a multipoint BET technique (NOVA 2000). The indexing of the x-ray diffraction patterns were carried out using the JCPDS (Joint Committee on Powder Diffraction Standards – International Centre for Diffraction Data, JCPDS-ICPDD) files. The line broadening analysis of the x-ray diffractograms and determination of the structure and lattice parameter were carried out using the software X-ray Diffraction Analysis (1992-93).

### 2.4.Leaching Experiments

The unmilled and activated samples were leached in a pyrex glass reactor fitted with thermometer at one end of the openings. The leaching experiments were carried out at 1% wt/vol in 50%

sulfuric acid. The temperature of leaching could be controlled to within  $\pm 2^\circ\text{C}$  by using a powerstat. The leaching experiments were carried out isothermally at different temperatures (80, 95 and  $120^\circ\text{C}$ ) and for various durations (30-240 min) in separate batch experiments. The samples were added after preheating the solution to  $40^\circ\text{C}$  and 5ml of leach solution is pipetted out at different leaching time. The Ti content in the solution was determined using a UV visible spectrophotometer (Shimadzu, Japan, Model No.160A) while that of Fe was determined using an Atomic Absorption Spectrophotometer (GBC Avanta). Calibration using standard solutions was done prior to the analysis.

### 3.RESULTS AND DISCUSSION

#### 3.1.Characterization

The optical microscopic results of unmilled sample shows sub-rounded to sub-angular grains of ilmenite with surface pits, etch marks/grooves and crescentic pits as seen in the fig.1. Reflected light microscopic studies of the sample suggest that ilmenite is the major phase along with trace amounts of hematite/ilmo-hematite. Many ilmenite grains were moderately altered and the alteration appears to have proceeded along grain boundaries, grain edges and fissures. The distribution of altered ilmenite in the sample is estimated to be around 10%.

The XRD result of unmilled and activated sample shown in fig.2 reveals traces of pseudo-rutile (JCPDS No.29-1494) with ilmenite (JCPDS No.29-0733) in chatrapur deposits. Chen (1997) suggested that ilmenite could be completely converted to metastable  $\text{Fe}_2\text{Ti}_3\text{O}_9$  (pseudorutile) and  $\gamma\text{-Fe}_2\text{O}_3$  phases after hundred hours of ball milling in air. Whereas the present study shows that psuedo-rutile peaks completely disappears after 4 hours of mechanical activation indicating the amorphisation of pseudo-rutile peaks. The effect of mechanical activation on the structural parameters was studied from line broadening and shifting of major ilmenite peaks. Variation of crystallite size and strain was calculated using Scherer's formula:

$$B_t^2 = \left[ \frac{0.9\lambda}{D \cos \theta} \right]^2 + [4\varepsilon \tan \theta]^2 + B_0^2 \quad (1)$$

Where,  $B_t$  is the full width at half maximum (FWHM) intensity of the peak,  $\lambda$  the wavelength of the radiation used,  $D$  is the average crystallite size,  $\varepsilon$  the strain,  $\theta$  the diffraction angle and  $B_0$  is the instrumental line broadening. Least square minimization of six major peaks of ilmenite yields crystallite size and stain. Figure 3 represents exponetial variation of crystallite size and linear variation of strain. Welham and Llewellyn (1998) discussed that decrease in crystallite size leads to increase in the grain boundary area, which has a greater effect on dissolution of ilmenite. Lattice parameters and lattice volume increases with the activation time (fig.4) within the experimental uncertainty. Increase in lattice constant and lattice volume indicates the structural disorder caused by mechanical activation.

The results of mean particle size and surface are shown in fig.5 indicate exponential variation with the time of activation. Welham and Llewellyn (1998) observed the reduction in surface area after 10 hours of milling by agglomeration of particles whereas in the present study the decrease in surface area was not observed upto 4 hours of planetary milling. The SEM micrograph (Fig.6.a, b) shows that mechanical activation produces predominantly angular shape of the powder particles, which enhances the dissolution rate (Tromans and Meech 1999 & 2002).

### 3.2. Leaching aspects

Table.1 represents the dissolution behavior of Fe and Ti in unmilled and activated samples. The unmilled and activated samples show sigmoidal variation of leaching. The leaching time decreases exponentially with the time of activation. The unmilled sample takes 3 hours to dissolve 50% Ti whereas 4 hours activated sample takes only 30 minutes at 120°C. It is observed that the dissolution of Fe is higher than that of Ti. XRD results of leach residues given in fig.7 represents ilmenite, rutile and ferrous titanium sulfate phases after leaching, which indicates Fe is leached differentially leaving behind TiO<sub>2</sub> in the leach residue and an intermediate phase Ferrous titanium sulfate is formed during leaching. The rate of the leaching reaction is enhanced by mechanical activation.

### 3.3. Kinetic aspects

The dissolution reaction of ilmenite in sulfuric acid leaching can be written as



The kinetics of dissolution is analysed with power law, diffusion models, phase boundary reaction, Avrami-Erofeev equation, autocatalysis models etc various models. But none the models could satisfactorily explain the dissolution behavior. A non-linear least squares minimization technique (Varhegyi et al., 2001) was therefore employed for the determination of the kinetic parameters for the dissolution of both Ti and Fe. For isothermal experiments, the basic kinetic equation can be given by:

$$g(\alpha) = \int_0^\alpha \frac{d\alpha}{f(\alpha)} = kt = A \exp\left(\frac{-E}{RT}\right)t \quad (2)$$

where  $\alpha$  is the fractional conversion,  $k$  is the rate constant ( $\text{min}^{-1}$ ),  $A$  is the pre-exponential factor  $E$  is the activation energy ( $\text{kJ/mol}$ ),  $R$  the gas constant ( $\text{kJ} \cdot \text{mol}^{-1} \cdot \text{K}^{-1}$ ) and  $T$  the absolute temperature ( $\text{K}$ ). In the present case, several functional forms for  $f(\alpha)$  were tried and the functional form of  $\alpha$  [ $f(\alpha)$ ] corresponding to  $n$ th order kinetics was found to be sufficient to describe the dissolution kinetics of both titanium and iron satisfactorily:

$$f(\alpha) = (1 - \alpha)^n \quad (3)$$

Since the Ti and Fe in the ilmenite dissolves differentially for the activated samples, and not according to their stoichiometry in the ilmenite phase, the dissolution kinetics of Ti and Fe has to be analyzed independently (Fig.8). The activation energy for the dissolution of Ti ranged from 53.9 to 62.0  $\text{kJ/mol}$  and that of Fe from 57.8 to 66.1  $\text{kJ/mol}$  depending on the time of milling. Further, the activation energies for the dissolution of both Ti and Fe decreased monotonically with activation time.

### 4. CONCLUSION

Mechanical activation introduces exponential variation of particle size, surface area, and crystallite size. The lattice parameters and volume of the unit cell were also increased by mechanical activation. All these factors contributed to the enhancement of dissolution rate of ilmenite. The Fe and Ti dissolve differentially not according to the stoichiometric proportion. The rate of dissolution of dissolution of Fe and Ti increases exponentially with the time of mechanical

activation. The results obtained by 100 hours of ball milling can be obtained by 4 hours grinding of ilmenite in a high energy-planetary milling.

#### ACKNOWLEDGEMENTS:

The authors are thankful to Sapan Das, T.C.Alex, Scientists, NML, Jamshedpur for the SEM and thermal analysis measurements respectively and Indian Rare Earths Limited, Chatrapur for supplying the ilmenite sample. The first author (CS) grateful to CSIR, New Delhi for providing a CSIR JRF fellowship for pursuing this work.

#### REFERENCES

- Amer A M 2000 *Hydrometallurgy* **58** 251
- Amer A M 2002 *Hydrometallurgy* **67** 125 Balaz P 1996 *Hydrometallurgy* **40** 359.
- Balaz P 2000 *Extractive Metallurgy of Activated Minerals*. Elsevier, Amsterdam.
- Balaz P, Ficeriova J, Sepelak V and Kammel R 1996 *Hydrometallurgy* **43** 367
- Chen Y 1997 *Jour of Alloys and Compounds* **257** 156
- Chen Y 1998 *Journal of Alloys and Compounds* **266** 150
- Sasikumar C, Rao D S, Srikanth S, Ravikumar B, Mukhopadhyay N K and Mehrotra S P 2004 *Hydrometallurgy* **75** 189
- Suresh Babu D S and Mohan Das P N 1999 *Trans. Indian Inst. Met.* **52** 73
- Tkacova K and Balaz P 1996 *Int. J. Mineral Process.* **44-45** 197
- Tromans D and Meech J A 1999 *Min. Engg.* **12** 609
- Tromans D and Meech J A 2002 *Min. Engg* **15** 263
- Varhegyi G, Szabo P, Jakab E and Till F 2001 *J. Analytical and Applied Pyrolysis* **57** 203
- Welham N J and Llewellyn D J 1998 *Min. Engg* **11** 827
- Welham N J 1997 *Trans. Inst. Min. Metall. Sec. C* **106** C138.
- Welham N J 2001 *Int. J. Miner. Process* **61** 145

#### FIGURE CAPTION:-

- Fig.1: Photomicrographs of the raw (unmilled) ilmenite concentrate sample under reflected light. Some of the ilmenite grains are unaltered (I) while some grains are altered along margins and cleavage planes( as shown by arrow marks).
- Fig.2: XRD of the unmilled sample and for various times of activation. (a - Unmilled sample; b - 30 minutes activated sample; c - 90 minutes activated sample and d - 240 minutes activated sample).

Fig.3: Variation of crystallite size and strain with activation time.

Fig.4: Variation of lattice parameter and unit cell volume with time of activation

Fig.5: Variation of mean particle size and surface area with time of activation.

Fig 6.SEM micrographs in the back scattered electron-imaging mode of the unmilled sample and activated sample: a) unmilled, b) 90 minutes activated.

Fig.7: XRD of leach residue of samples activated for various times and leached at 120°C (a - leach residue of unmilled sample, 60 min leaching time; b – leach residue of unmilled sample, 240 min leaching time; c - leach residue of sample activated for 240 minutes, 240 min leaching time).

Fig.8:Variation of activation energy for the dissolution of Ti in sulphuric acid with activation time.

(b)Variation of activation energy for the dissolution of Fe in sulphuric acid with activation time.

Table.1. Leaching results of Ilmenite dissolved in 50% H<sub>2</sub>SO<sub>4</sub>

Time of activation	Time of leaching	%Ti dissolved			%Fe dissolved		
Minutes	Minutes	80 <sup>0</sup> C	95 <sup>0</sup> C	120 <sup>0</sup> C	80 <sup>0</sup> C	95 <sup>0</sup> C	120 <sup>0</sup> C
0	30	1.68	4.00	32.13	0.81	1.28	22.62
“	60	4.25	10.30	41.65	1.82	3.68	35.79
“	120	7.99	19.23	49.05	3.63	7.88	38.67
“	180	11.17	23.84	52.19	5.50	10.99	40.77
“	240	11.99	26.15	53.25	6.71	13.01	42.38
30	30	13.21	18.89	38.83	5.06	8.40	34.41
“	60	19.60	25.36	47.42	8.65	12.95	42.72
“	120	26.42	31.74	54.48	12.81	18.40	46.08
“	180	30.82	35.61	55.67	16.09	22.24	48.18
“	240	33.05	37.49	56.77	18.14	24.29	49.79
90	30	21.20	25.36	46.23	9.39	17.78	53.02
“	60	27.58	31.74	52.88	16.10	23.61	60.58
“	120	36.58	39.77	58.37	24.91	32.05	71.43
“	180	37.81	42.00	58.84	28.30	34.56	74.37
“	240	38.80	43.60	60.07	30.79	36.25	75.61
240	30	24.04	38.46	51.87	24.34	30.01	72.23
“	60	30.91	46.55	59.59	30.70	38.12	82.90
“	120	41.65	50.80	63.47	37.00	44.75	88.98
“	180	43.13	51.87	64.53	39.16	47.30	93.53
“	240	45.44	51.80	65.22	39.72	48.84	95.01





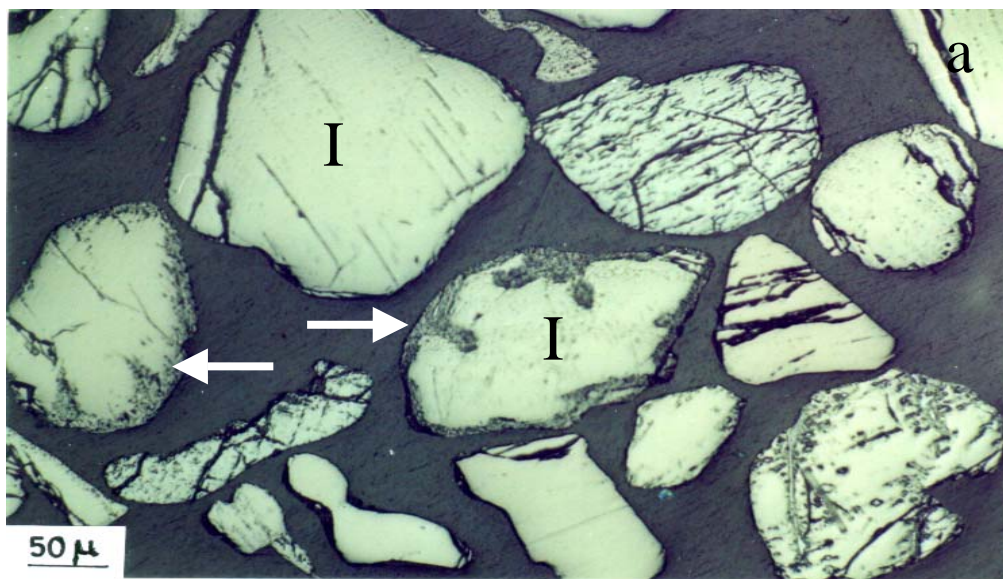


Fig.1

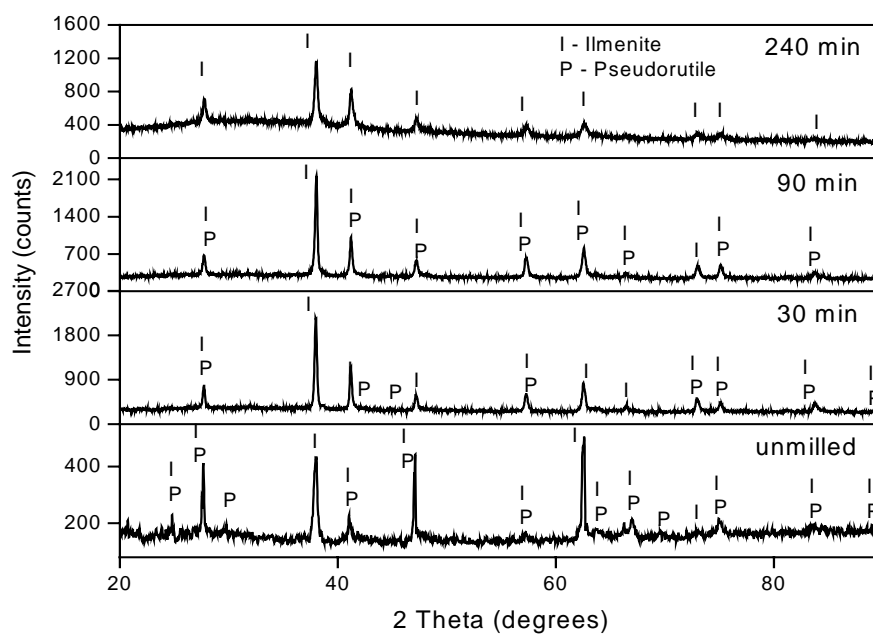


fig.2

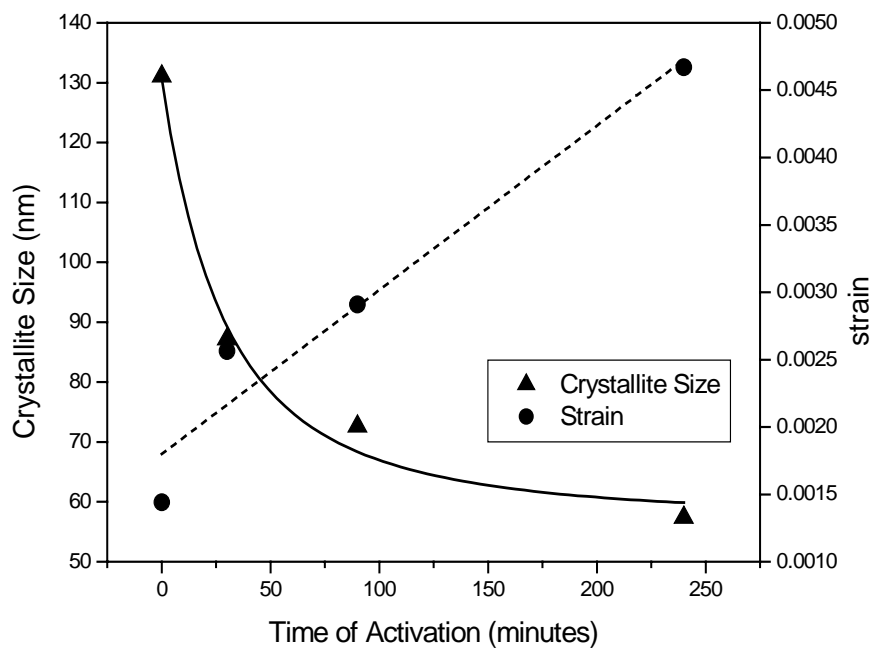


fig.3

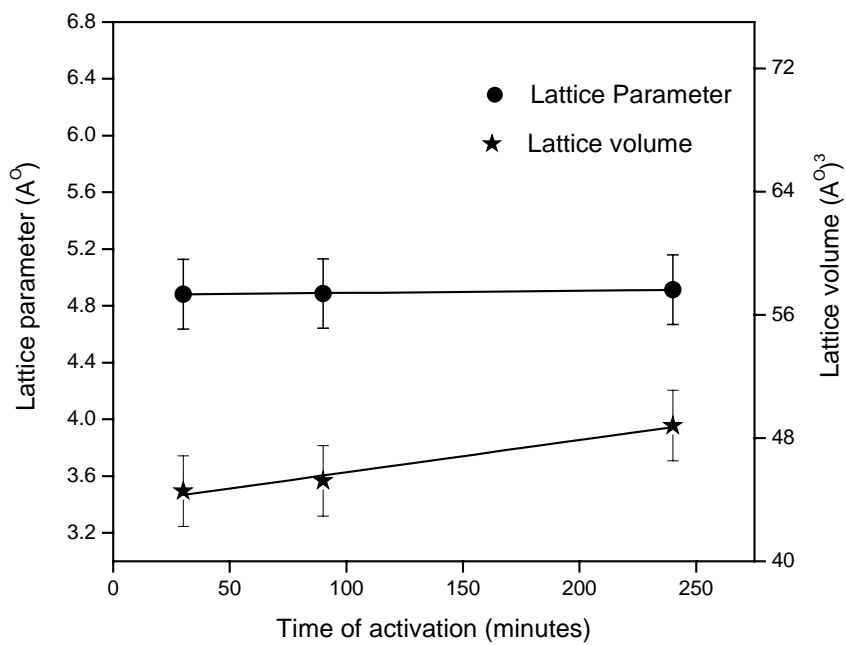


fig.4

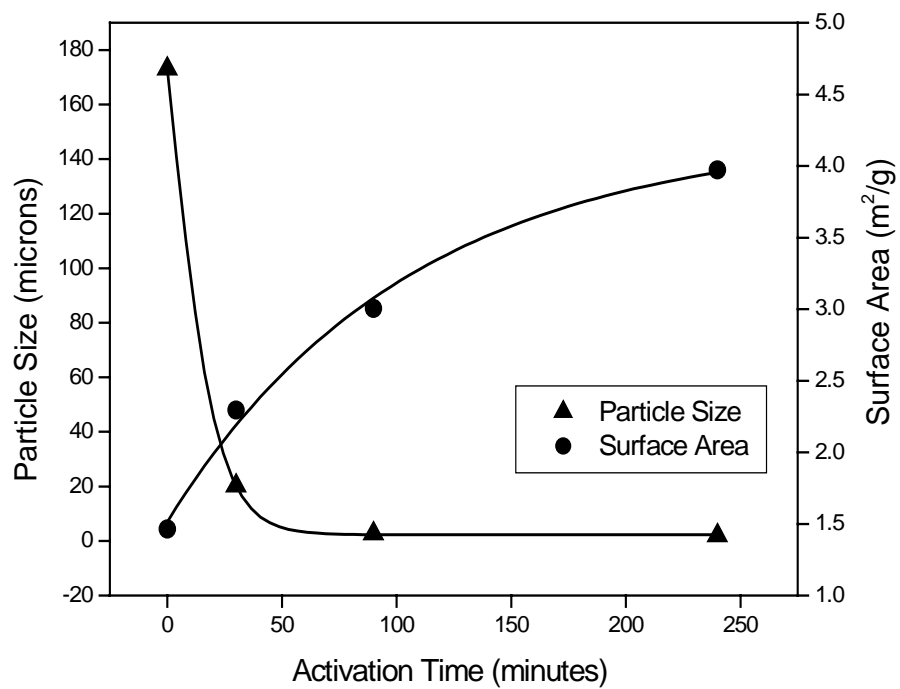


fig.5

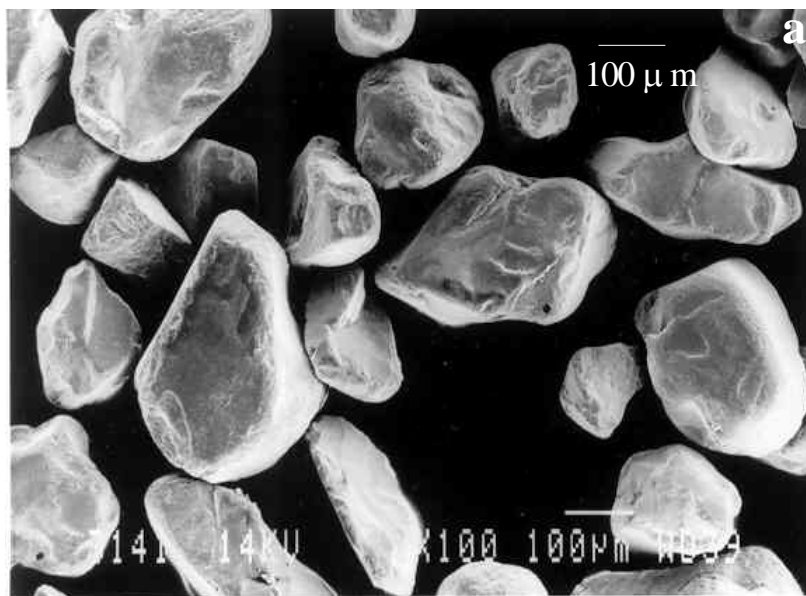


fig.6a

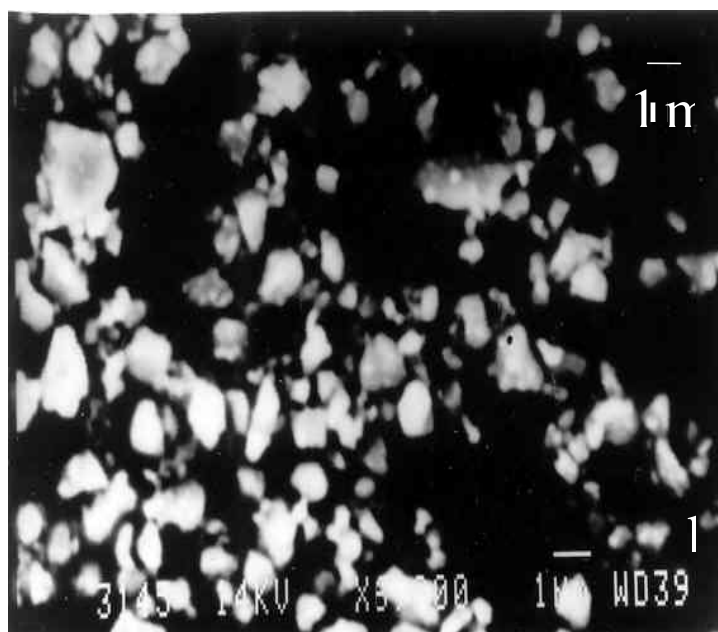


Fig.6b

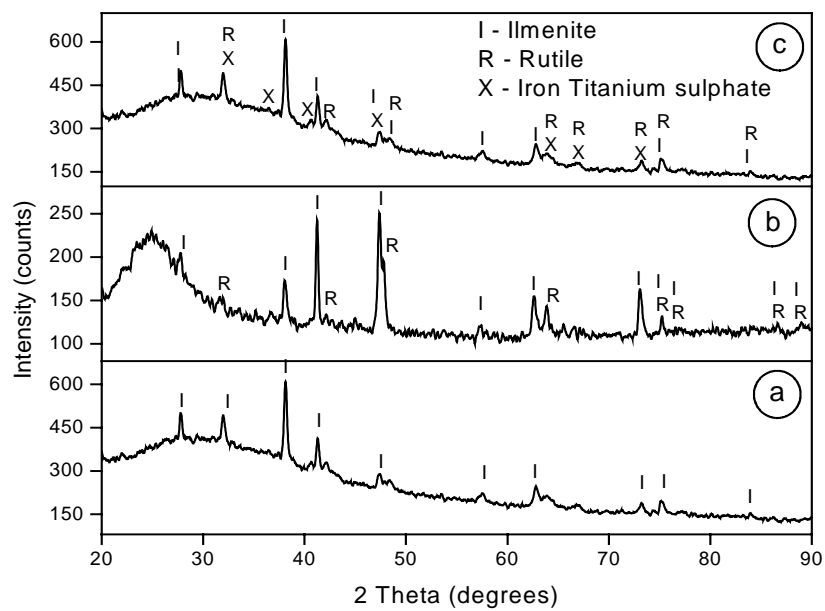


Fig.7

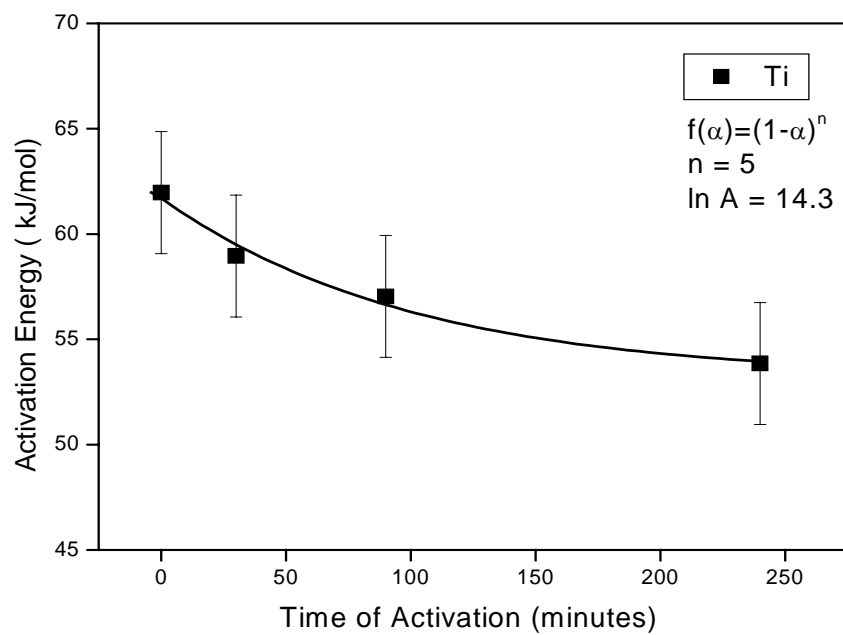


fig.8a

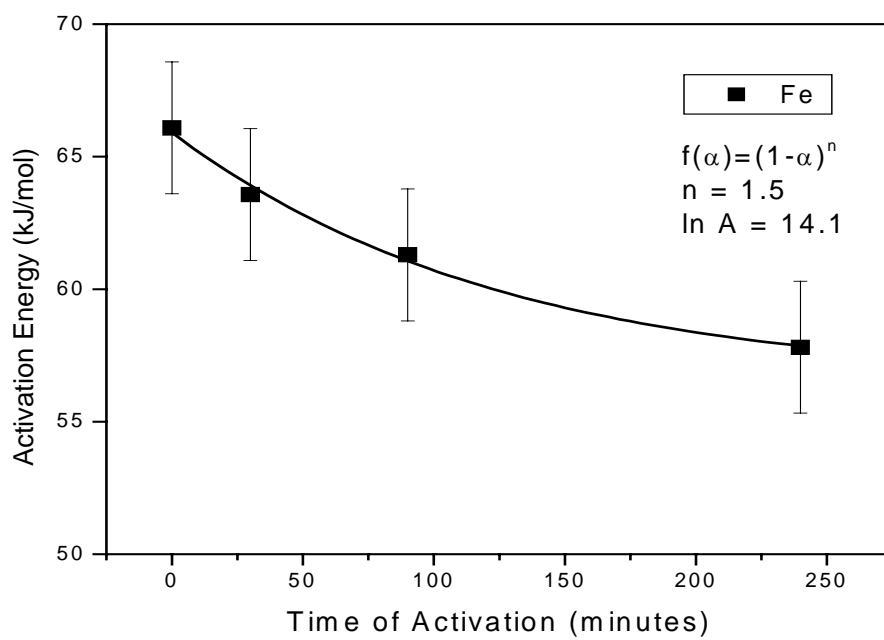


fig.8.b